172–181 *Nucleic Acids Research, 2010, Vol. 38, No. 1* *Published online 23 October 2009*
doi:10.1093/nar/gkp884

Understanding how the crowded interior of cells stabilizes DNA/DNA and DNA/RNA hybrids–*in silico* predictions and *in vitro* evidence

Karthik S. Harve[1,2], Ricky Lareu[1,3,4], Raj Rajagopalan[2,5] and Michael Raghunath[1,6,*]

[1]Tissue Modulation Laboratory, Division of Bioengineering, Faculty of Engineering, National University of Singapore, Singapore 117510, [2]Singapore-MIT Alliance, E4-04-10, 4 Engineering Drive 3, NUS, Singapore 117576, [3]NUS Tissue Engineering Program, Life Science Institute, NUS, 117510, [4]Molecular Hepatology, School of Medicine and Pharmacology, Faculty of Medicine, Dentistry and Health Sciences, The University of Western Australia, [5]Department of Chemical and Biomolecular Engineering, Block E5, 4 Engineering Drive 4, National University of Singapore, Singapore 117576 and [6]Department of Biochemistry, Yong Loo Lin School of Medicine, National University of Singapore, Singapore

Received August 19, 2009; Revised October 1, 2009; Accepted October 2, 2009

ABSTRACT

Amplification of DNA *in vivo* occurs in intracellular environments characterized by macromolecular crowding (MMC). *In vitro* Polymerase-chain-reaction (PCR), however, is non-crowded, requires thermal cycling for melting of DNA strands, primer-template hybridization and enzymatic primer-extension. The temperature-optima for primer-annealing and extension are strikingly disparate which predicts primers to dissociate from template during extension thereby compromising PCR efficiency. We hypothesized that MMC is not only important for the extension phase *in vivo* but also during PCR by stabilizing nucleotide hybrids. Novel atomistic Molecular Dynamics simulations elucidated that MMC stabilizes hydrogen-bonding between complementary nucleotides. Real-time PCR under MMC confirmed that melting-temperatures of complementary DNA–DNA and DNA–RNA hybrids increased by up to 8°C with high specificity and high duplex-preservation after extension (71% versus 37% non-crowded). MMC enhanced DNA hybrid-helicity, and drove specificity of duplex formation preferring matching versus mismatched sequences, including hair-pin-forming DNA- single-strands.

INTRODUCTION

Macromolecular crowding (MMC) is a ubiquitous biophysical feature of the cellular interior and governs all biochemical reactions therein (1). Rough estimates of MMC in terms of solids in solution range from 300–400 mg/ml in *Escherichia coli* (2), over 50–400 mg/ml in eukaryotic cytoplasm (1), 270–560 mg/ml in mitochondria (2) and 100–400 mg/ml in nuclei (3). Through creating an excluded volume effect, MMC drives polymer folding into native states (4,5), thus enhancing enzyme kinetics (6) and the formation of supramolecular assemblies (7). Remarkably, only one study to date has shown indirect evidence that also nucleotide associations are stabilized by MMC (8). Whether at ambient or body temperature, DNA polymerization in prokaryotes and eukaryotes occurs under crowded conditions and is enzymatically controlled. *In vivo*, the first step of DNA polymerization is facilitated by helicases and associated proteins wedging themselves into the DNA double strands, thereby breaking hydrogen bonds between complementary bases (9,10). In the absence of helicases *in vitro*, DNA polymerization of mammalian DNA with mammalian polymerases and associated proteins at body temperature (37°C) is very tardy (11). This problem was overcome with the advent of PCR, an *in vitro* DNA amplification method that generates billions of DNA copies from a single starting molecule within a short time. PCR is based on the cyclic application of heat in three phases. First, to

*To whom correspondence should be addressed. Tel: +65 6516 7657, extn 5307 (DSO building); Fax: +65 6872 3069; Email: bierm@nus.edu.sg

The authors wish it to be known that, in their opinion, the first two authors should be regarded as joint First authors.

© The Author(s) 2009. Published by Oxford University Press.
This is an Open Access article distributed under the terms of the Creative Commons Attribution Non-Commercial License (http://creativecommons.org/licenses/by-nc/2.5/uk/) which permits unrestricted non-commercial use, distribution, and reproduction in any medium, provided the original work is properly cited.

substitute for helicase activity, the DNA double helix is thermally separated into single strands, typically at 95°C. Then the temperature is lowered 50–55°C to allow for the subsequent annealing of short, complementary primers (~18–20 nucleotide oligomers) to these exposed single-strands - a highly random and entropy-driven process (12). Lastly, the enzymatic extension of primers to create a complementary strand is performed by polymerases derived from thermophilic bacteria at 68–72°C. As this clearly exceeds the optimal annealing temperature the bound primer-template complexes are predicted to dissociate in the extension phase, which will stunt PCR yield from the very first cycle onwards (13). We have recently demonstrated that MMC leads to faster amplicon yields and increased specificity of the PCR reaction (14). We initially attributed the results to the fact that MMC protects *Taq* polymerase against heat denaturation, a finding that ties in with earlier findings of MMC effects on other proteins (4). Earlier work (15) has shown stabilization of higher temperature states involving hair-pin forming protein chains under confinement. However, we noticed that little is known about the effects of MMC on DNA/DNA and DNA/RNA hybrid formation and wondered to what extent the observed MMC effects in PCR are related to stabilization of hybrid formation in the extension phase which would explain the dramatically increased yield and faster reaction rate in real-time PCR.

We therefore used a combined *in silico*/*in vitro* approach to address this question and show that atomistic simulations indeed predict a stabilization of hybrids via preservation of hydrogen bonds and structure, which is reflected *in vitro* by dramatic melting temperature rises of DNA/DNA and DNA/RNA hybrids with a manifold increase in duplex formation and a remarkable preference for matching sequences over mismatches and hair pins.

MATERIALS AND METHODS

Molecular dynamics simulations

Single-molecule MD simulations were done on DNA and RNA hybrids in the Discovery Studio™ Molecular Simulations package with CHARMm force-field. Solvent (water) was simulated in an implicit solvent model (Generalized Born). More details on the simulations are explained in supplementary section. Briefly, initial energy minimization was done with Steepest Descent Algorithm (10 000 steps) and dynamics cascade carried out in sequential steps (1.0 fs steps) of heating [target temperature: 307K (34°C); 100 000 steps], equilibration (800 000 steps) and production (100 000 steps) for a total of 1 ns. Oligo DNA simulated were the following sequences 5′-A_{20}-3′: 5′-T_{20}-3′, 5′-A_{15}-3′: 5′-T_{15}-3′, 5′-AAT CAG TTA GTA ATT CAT TC -3′: 5′-GAA TGA ATT ACT AAC TGA TT-3′. For experiments on DNA:RNA hybrids, oligo DNA 5′-T_{20}-3′: oligo RNA 5′-rA_{20}-3' hybrids were simulated. MMC were set-up on a confinement platform by encaging the DNA in polymeric chains of α-D-1,6-Glucose (15 kDa). The rationale of designing the confiners is explained in results section. Stability of DNA-duplex was determined by monitoring the H-bonding between the DNA–DNA or DNA–RNA strands as well as the RMSD (root-means-squared-displacement) of the structures (centres of mass of all atoms) after the simulation runs under confined (crowded) or non-confined (non-crowded) conditions for three independent runs and the averages were computed as mentioned before.

Real-time measurement of DNA hybridization

Oligo DNA sequences 5′-A_{20}-3′: 5′-T_{20}-3′, 5′-A_{15}-3′: 5′-T_{15}-3′, 5′-AAT CAG TTA GTA ATT CAT TC-3′: 5′-GAA TGA ATT ACT AAC TGA TT-3′, 5′-T_4A_{16}-3′: 5′-$T_{16}A_4$-3′, 5′-A_4T_{16}-3′: 5′-$A_{16}T_4$-3′ (1st Base, Singapore unless specified otherwise), all at final concentrations of 1.0 μM, were dissolved in a 10× PCR reaction buffer (final concentrations of 20 mM Tris and 50 mM KCl, 3 mM $MgCl_2$) and 20× SYBR Green I (SG I; Molecular Probes) in a 20 μl reaction volume. The oligomers were hybridized under PCR-typical temperatures in steps of 95°C/30s, 50°C/1 min, 72°C/30s, on a real-time thermal cycler (Stratagene, USA) for 1, 4 or 40 cycles, followed by a dissociation run from 50°C → 94°C. Oligomers with SNPs in their sequence 5′-A_{10}-C-A_9-3′ (sequence ID:MS-1) were co-incubated with 5′-T_{20}-3′ and 5′-T_{10}-C-T_9-3′ (ID:MS-2) with 5′-A_{20}-3′ in reaction buffer ± MMC. For experiments on DNA-RNA hybrids, oligo DNA 5′-T_{20}-3′: oligo RNA 5′-rA_{20}-3′ (Sigma-Aldrich) and SYBR Green I (20×) were dissolved in water or MMC solution, heated at 65°C/5 min and cooled on ice as in the first step of a reverse transcription. Then the 5× first strand buffer (final concentrations of 50 mM Tris, 75 mM KCl, 3 mM $MgCl_2$) was added to the oligo mix kept on ice and then heated at 42°C/50 min → 70°C/15 min. Macromolecular crowders used were Ficolls 70 and 400 (Fc70, Fc400; Amersham), Ficoll 400 and polyvinyl pyrrolidone 360 (PVP360; Sigma). Fc400 as mono-crowder was used at final concentration of 40 mg/ml and in combination, the final concentrations of Fc70, Fc400, PVP360 were 15 mg/ml, 5 mg/ml and 500 μg/ml, respectively. Area under the melt curves (AUC) were computed using the NCSS™ Software (www.ncss.org). For theoretical estimates on melting temperature, Oligo Analyzer™ online software was used. Experiments were done in duplicates for three independent runs and average values computed. Statistical significance was estimated by a Student's *t*-test ($P < 0.05$).

Dynamic light scattering analyses of crowder solutions

The set-up for Dynamic light scattering (DLS) experiments to study the effects of PVP360 on the aggregation behavior of Fc70 is described in Supplementary Data 3S.

Circular Dichroism spectroscopy experiments

Oligo DNA with the following sequences 5′-A_{20}-3′: 5′-T_{20}-3′ (1st Base, Singapore), all at final concentrations of 1.0 μM, were dissolved in a 10× PCR reaction buffer at 700 μl reaction volumes with or without MMC (Fc70/Fc400/PVP360 as given above). Blanks were set up without DNA in the solution. UV-Visual Circular

Dichroism (CD) spectra of the reaction mixes were recorded in a Jasco-810^{TM} Spectropolarimeter between 200 and 300 nm wavelengths. DNA CD Spectra normalized against blanks were recorded at 25°C, 95°C, 50°C, 72°C in that order for each set of reaction mixes. Experiments were done in duplicates for three independent runs and averages computed. Statistical significance was estimated by a Student's *t*-test ($P < 0.05$).

RESULTS

Computational modelling reveals that macromolecular confinement stabilizes double-stranded DNA structure against heat and facilitates hydrogen bond formation

We set up simulation experiments on a Molecular Dynamics platform (total duration 1 ns using CHARMm forcefield) by confining single molecule DNA duplices within carbohydrate polymeric structures. The simulation cascade comprised of three subsequent phases, the heating, equilibration and production phases, respectively. The heating and equilibration phases were carried out at target temperature of 307 K (34°C) and the readouts were collected in the production phase at the same temperature (see Supplementary sections 1S and 2S). After initial minimization of the starting configurations of 20 base-pair oligo-DNA (A_{20}:T_{20}), the maximum H-bond number is 40. The initial structures were set as reference to calculate the average Root-Means-Squared-Displacement (RMSD) of the centres of mass (of all atoms) of the simulated structures from the initial conformations. Comparison of the simulation output at the end of 400 ps with that at the end of 800 ps under both non-crowded and confined/MMC conditions showed negligible potential energy difference suggesting that equilibrium had been reached at a target temperature of 34°C (Supplementary Figure S2). Additional theoretical analyses and calculations suggested that in this simulation system the macromolecular crowders have a much slower diffusion velocity than nucleotide oligomers (Supplementary Table S1). Therefore, the crowders can be regarded as static in relation to DNA hybrids and thus confining them within. At the end-equilibration stage after heating to 34°C, the two strands separated completely during the production phase (number of H-bonds = 0; Figure 1a). Under confinement conditions, however, the model predicted that there was still an average of 11 of the original 40 H-bonds intact (Figure 1b). RMSD values showed for control conditions, a mean of 21.6 nm from the initial structure for the final structure. Under confinement, the mean RMSD was 8.325 nm, confirming far less thermal disruption of the hybrid.

In silico confinement models predict structural stabilization of nucleic acids of different conformations at elevated temperatures

We applied *in silico* simulations to predict the dissociation behaviour of different nucleic acid hybrids; length, sequence, type (of hybrids) and conformation (Table 1). After initial minimization of the starting configurations of 15 base-pair oligo-DNA (A_{15}:T_{15}), the maximum number of H-bonds was 30. At the end-equilibration stage, under non-confined conditions, the individual strands

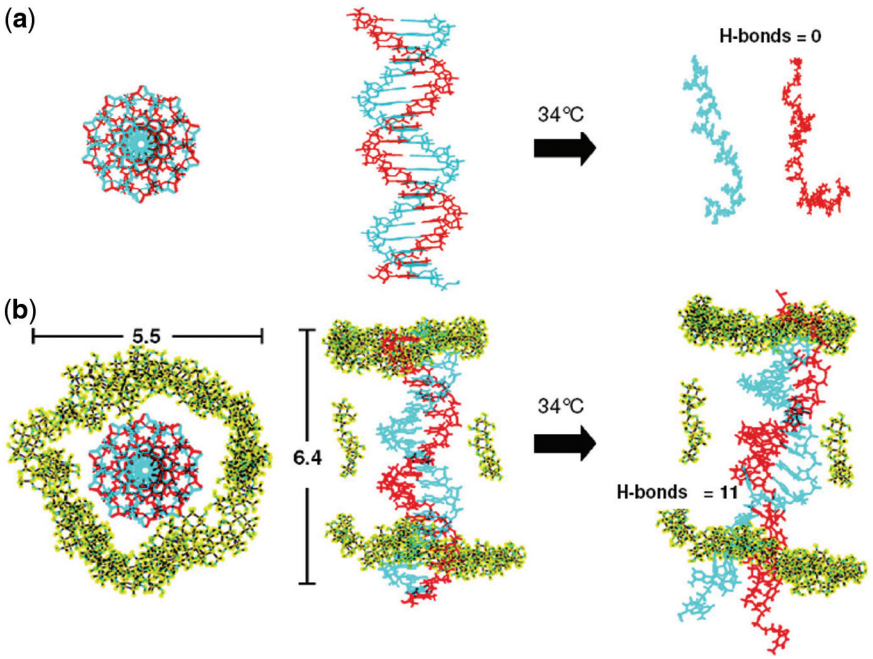

Figure 1. Snapshots of simulated single DNA–DNA hybrid from a 1 ns-Molecular Dynamics run: (**a**) MD simulations of DNA denaturation by heating to 307K (34°C) breaks all the 40 H-bonds of the double helix. However, a confined environment (**b**) modelled as dough-nut shaped rings surrounding the two ends of the duplex and two chains as sidewalls, the dimensions (in nm) as shown in the figure, maintains the double helical structure by retaining 11 of the original 40 H-bonds.

Table 1. Summary of MD Simulations shows that Macromolecular Confinement preserves H-bonding between complementary duplexes and this is a generic effect for nucleic acid hybrids of different lengths, conformations and sequence

Nucleic Acid type	After heat treatment			
	H-bonds		RMSD (nm)	
	UC	MMC	UC	MMC
DNA:DNA(A_{15}:T_{15})	0	6	19.02	8.66
DNA:DNA(random)	0	4	20.0	9.6
DNA:RNA(dT_{20}:rA_{20})	0	15	11.0	8.18

of the DNA hybrid separated completely (number of H-bonds = 0). Under confinement conditions, however, an average of six of the original 30 H-bonds was still intact. Accordingly, the final structure showed a mean RMSD of 19 nm and 8.6 nm under unconfined and confined conditions respectively, from the initial structure. Thus, the model predicted that confinement also stabilizes shorter DNA duplexes against heat. We then tested if MMC could stabilize DNA oligomers of random sequences. At the end-equilibration stage, under confinement, there were still 4 of the original 45 H-bonds intact final structure showed a mean RMSD of 20 nm and 9.6 nm under unconfined and confined conditions respectively, from the initial structure. The average number of H-bonds for the random sequence after the simulations is slightly lower than that for poly A: poly T sequences. However, statistical analysis showed that this difference was not significant ($P < 0.05$). The effects of confinement were then tested on DNA:RNA hybrids (20 nt). Initial simulations runs identified a target temperature of 290K (17°C) as sufficient to break all the H-bonds between the DNA:RNA hybrids under unconfined conditions (Table 1). At this temperature the simulated DNA:RNA hybrids under confinement show 15 of the original 40 H-bonds intact. Thus, confinement stabilizes DNA:RNA against heat-induced denaturation.

MMC *in vitro*: hierarchy of complexity in stabilizing DNA–DNA duplices

The melting temperature profile of DNA/DNA hybrids as assessed with a dissociation run under real-time thermal cycling conditions correlated with increasing complexity of the crowding solution (Figure 2). Mono-crowding with Fc400 increased the melting point of the hybrid DNA by an average of 1 ± 0.2°C, whereas the binary Fc mix resulted in an average 1.5 ± 0.1°C shift. However, adding PVP360 to the Fc mix raised the melting point by an average of 7.6 ± 0.78°C (Figure 2). Changes of the area under the melt curve (AUC; which is a computational estimate of the population of duplex DNA just before dissociation) indicated a 3-fold increase of preserved duplexes with monocrowding, whereas a mixed crowder cocktail increased the duplex population by 6-fold over non-crowded control. Real-time monitoring of nucleic acid hybrid formation and thermal stability demonstrated that MMC also worked across different fragment lengths and conformations [DNA 15-mers, random sequence DNA fragments (20-mers) and DNA:RNA] (Table 2). Again, the ternary mix of macromolecular crowders proved to be the most efficacious in raising the melting temperatures of hybrids. Based on these findings, all further experiments were done with the ternary mix of crowders.

To study the behaviour of macromolecular crowders in mixed MMC, we analysed a pure solution of Fc70 by DLS. A uniform size distribution was evident with an average hydrodynamic radius of 5.2 nm (Supplementary Figure S3a). In the presence of PVP360 the Fc70 size distribution showed an additional distinct population with an average of 9.4 nm suggesting multimerization (Supplementary Figure S3b).

Mixed MMC enhances specificity of hybridization and thermal stability of nucleic acids in straight and hairpin conformation

MMC did not promote annealing of mismatched oligonucleotides or stabilization of mismatched hybrids (Figure 3a), but preferably stabilized perfect matching hybrids (Figure 3b). When matching and mismatching hybrids were co-incubated, the formation of perfectly matched hybrids was greatly enhanced under crowding in preference over mismatched hybrids as evident by a 15-fold increment in the duplex-DNA population with a much higher duplex-melting-temperature than the mismatched hybrids (by 10°C). Further, the dissociation curves for mismatched hybrids under crowding and uncrowded conditions were identical and overlapped each other, indicating no difference in melting behaviour (Figure 3a). In a separate set of experiments, oligo DNA 20-mers were designed to form hair-pin structures due to internal base-pairing between the complementary nucleotides within their sequence. When such oligomers were co-incubated with their complementary sequence nucleotides (which also similarly could form hair-pin structures) under non-crowded conditions, the melting peaks showed a negligible fluorescence signal (Figure 3c) due to a small duplex population as indicated by the AUC (1094 sq. units). In contrast, MMC lead to a clearly detectable fluorescence signal due to abundant duplex population, AUC = 20 833 sq. units, a ~20-fold increment and with an increase in melting temperature of 5.0 ± 0.6°C compared to the non-crowded condition. The 20 bp length of the hybridized products was confirmed by 4% Agarose gel electrophoresis (Supplementary Figure S4). Appropriate controls were run to visualize the SG I fluorescence when only one set of oligomers were present in the solution without its complementary pair so that the oligomer formed a hairpin structure and no fluorescence was detectable due to absence of duplexes.

CD confirms thermal stabilization of DNA double helices by Mixed MMC

Under both control and MMC the UV-Visual CD Spectra (mdeg) of a double-stranded DNA hybrid of oligo

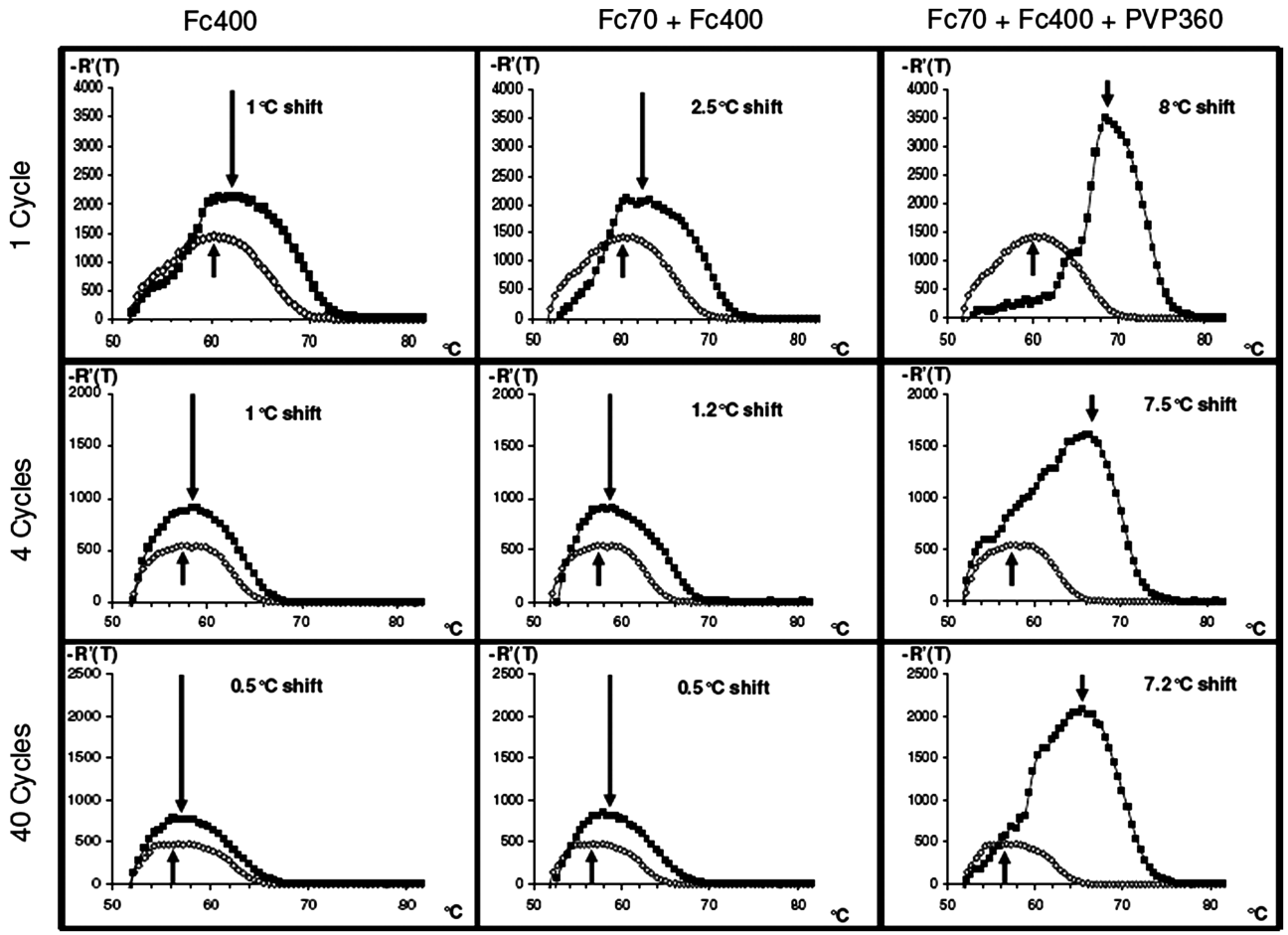

Figure 2. Dissociation Curves of 20-oligonucleotide DNA-DNA hybrids under non-crowded (open square) and crowded (filled square) conditions. MMCs applied were Fc400 alone, Fc400 + Fc70 and Fc400 + Fc70 + PVP360 and dissociation curves obtained after 1, 4 and 40 cycles in each condition. Fc400 and the Ficoll binary mix show shifts of 0.5–2.5°C and adding PVP360 to the binary mix increased the shift in the range of 7–8°C at the three cycle conditions. Area under the melt curves (AUC) were computed to show an average of 3- and 6-fold increase in the DNA population for single and mixed (ternary) crowding respectively over and above the uncrowded conditions.

Table 2. Real-Time monitoring of thermal stability shows that the effects of Crowding are generic for nucleic acid hybrids of different lengths, conformations or sequence

Nucleic Acid	Fluorescence (RFU)				Melting peak shift (°C)
	Annealing		Extension		
	UC	MMC	UC	MMC	
DNA(A_{15}:T_{15})	13900	58704	2523	3537	7.0
DNA(random)	19570	51760	2572	5031	6.4
DNA:RNA	65°C/5 min		42°C/50 min		Melt shift (°C)
	2700	3100	17506	62271	5.4

(dT): oligo (dA) gave a typical read-out at 25°C as described for the B-conformation of the DNA double helix at this temperature (16), namely a positive peak at 260 nm, and a negative trough at 247 nm (Figure 4a). At 95°C, total reduction of signal in both control and MMC (Figure 4b), indicated complete denaturation of DNA into single strands. At 50°C the CD spectra of controls and MMC were similar (Figure 4c) without significant difference at 260 nm or 247 nm. At the extension temperature of 72°C non-crowded controls showed a shallower 247 nm trough in comparison to 50°C (Figure 4d) with a decreased 260 nm peak. In contrast, the 260 nm peak persisted under MMC and the 247 nm trough deepened significantly ($P < 0.05$).

Mixed MMC stabilizes double-stranded DNA cyclic temperatures of a typical PCR

Real-time measurements showed a dramatic stabilization of DNA–DNA hybrids in the first and later cycles (Figure 5). During the first cycle, after the annealing phase, when the temperature is raised to 72°C (the PCR extension temperature), under non-crowded conditions, there was a steep drop in the number of duplex DNA to 37% of the initial population annealed under non-crowded conditions. However, under crowding at the extension temperature, 71% of the duplex DNA remained (Figure 5). The crowding effects resulted in a 2-fold increase of duplex DNA at annealing and 4-fold

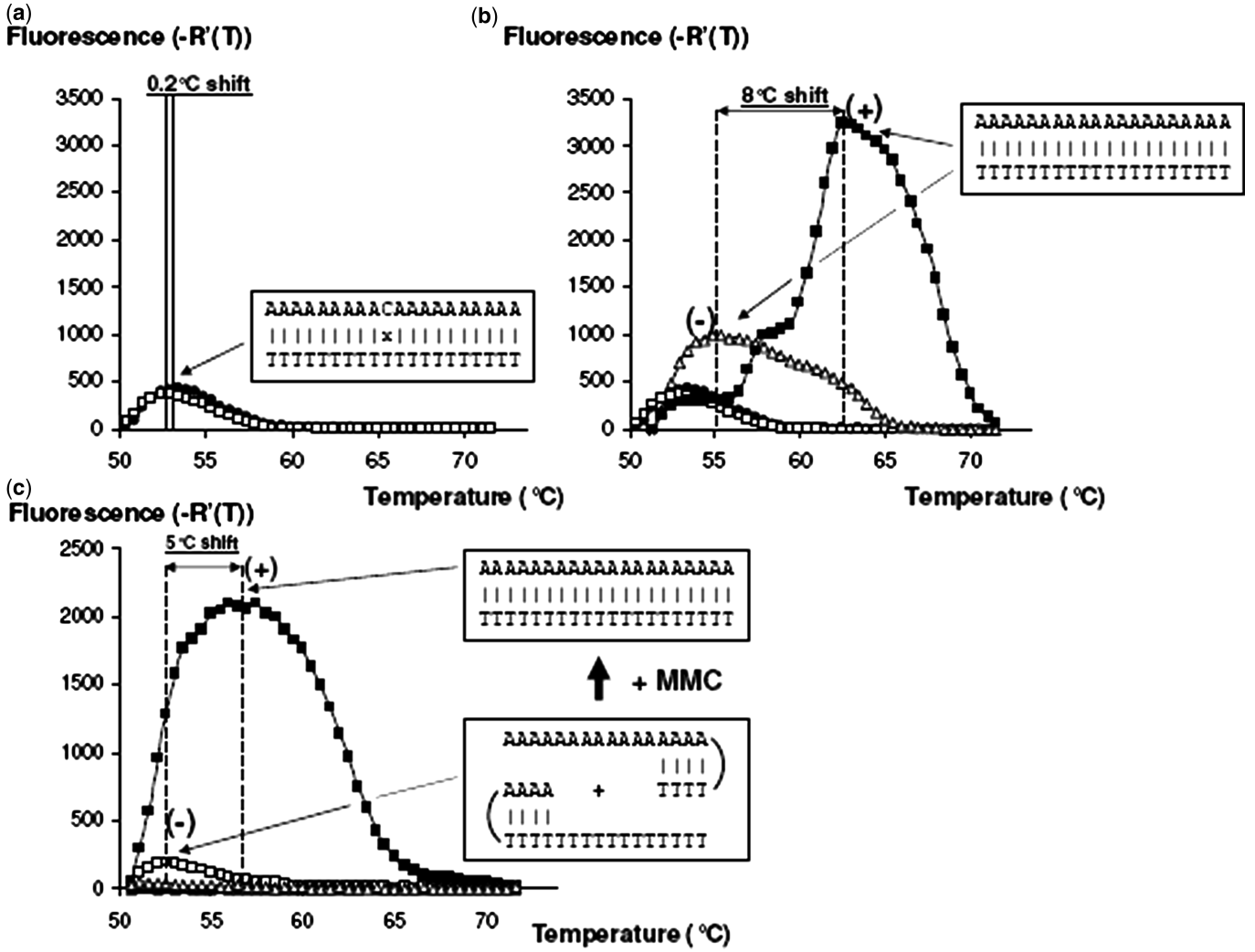

Figure 3. Dissociation curves of DNA duplexes between mismatched oligo(20)-mers ± MMC. In each panel, *x*-axis represents temperature (°C) and *y*-axis represents fluorescence intensity [-R'(T)]. (**a**) The melt curve when mismatched oligomers were co-incubated with 5′-T_{20}-3′ under uncrowded (open square) and MMC (filled circle). Note that there is a near complete overlap of the uncrowded and crowded melt curves for the mismatches indicating that there was no non-specific enhancement of binding of these mismatched DNA under MMC. (**b**) The same experiment with the addition of the positive controls: the 5′-A_{20}-3′: 5′-T_{20}-3′ hybrids at uncrowded (open triangle) and MMC (filled square). Note that in such a reaction mix, there is preferential formation of true matches under crowding with an 8°C higher melting temperature. (**c**) Dissociation Curves of 20-mer hair-pin DNA-DNA hybrids under non-crowded (open square) and crowded (filled square) conditions. The non-crowded condition shows a weak fluorescence due to a sparse duplex population, whereas under crowded condition, the fluorescence is well detectable suggesting a rich duplex DNA population. Area under the curves showed almost a 20-fold increase in DNA population duplex formation under crowded compared to non-crowded conditions (20883 versus 1094 sq. units, respectively).

at extension phase over the non-crowded after cycle 1. The crowding effects were more pronounced at later cycles, with a 4-fold increase at annealing (at both 4 and 40 cycles) along with a 6-fold and 8-fold increase at extension, after 4 and 40 cycles, respectively (Figure 5). All increases observed under MMC at annealing and extension were statistically significant ($p < 0.05$). Thus, at both the end-annealing and end-extension phases, the crowded condition resulted in higher fluorescence due to a greater amount of duplex DNA.

DISCUSSION

Our work demonstrates the enormous efficacy of macromolecular crowding on nucleotide hybridization events. This is the first *in silico* study on DNA/DNA and DNA/RNA hybridization under confined conditions. Atomistic modelling allowed us to obtain two pieces of important information. First, confinement can in fact stabilize nucleotide hybridization thereby facilitating H-bond formation and a nucleotide double-helix irrespective of length, sequence or type. This assisted us greatly in designing respective wet lab experiments.

Second, in keeping with previous reports (17,18) we recognized the role of diffusion velocities of crowding molecules versus crowded targets. We noted that differences in diffusion velocity actually lead to a quasi-static confinement situation adding a new facet to crowding theory. When in solution, DNA diffuses (diffusion-coefficient: $9.8 \times 10^{-7}\,cm^2/s$) an order of

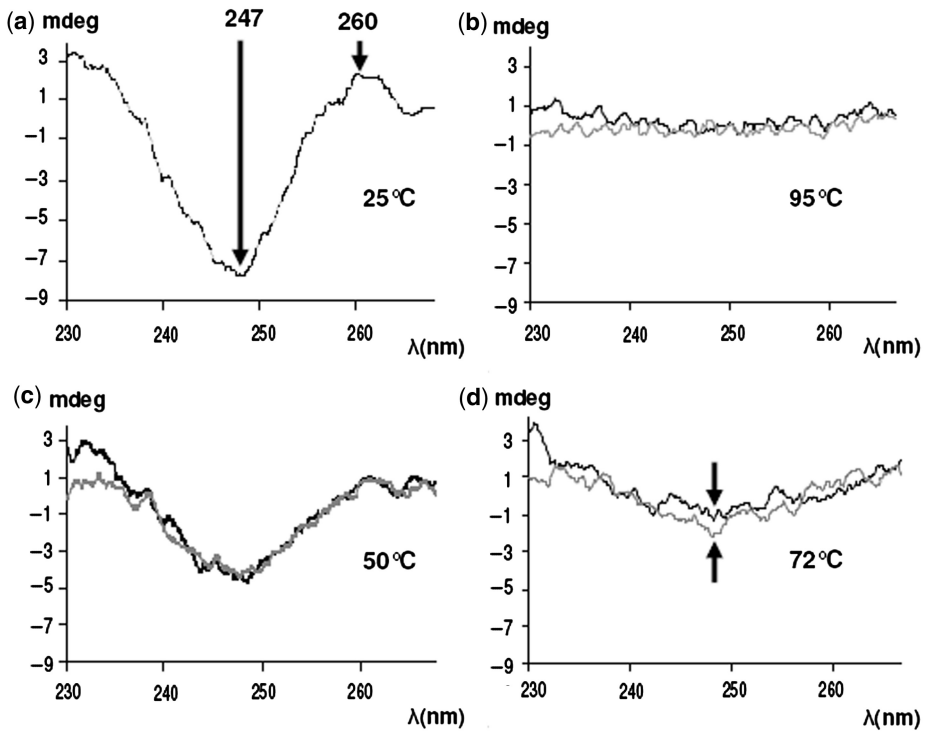

Figure 4. UV-Vis Spectra of oligo (dT): oligo (dA) in buffer under standard (non-crowded; black curves) and crowded (grey curves) conditions. (**a**) A CD spectrum of the B-form DNA at 25°C showing a positive peak at 260 nm and negative trough at 247 nm. (**b**) At 95°C, all DNA is in single-stranded conformation due to denaturation. (**c**) At annealing, both crowded and non-crowded conditions show similar spectra. Note that the exaggerated peak at 260 nm seen at room temperature disappears. (**d**) At 72°C, the peak at 260 nm persists for the crowded condition, whereas it disappears in the non-crowded indicating that the duplex has melted away. The much deeper trough at 247 nm in MMC than the non-crowded by a mean mdeg of 0.8 unit [which was statistically significant ($P < 0.05$); see arrows in d] suggests that there is still a double helical secondary structure present under MMC at 72°C.

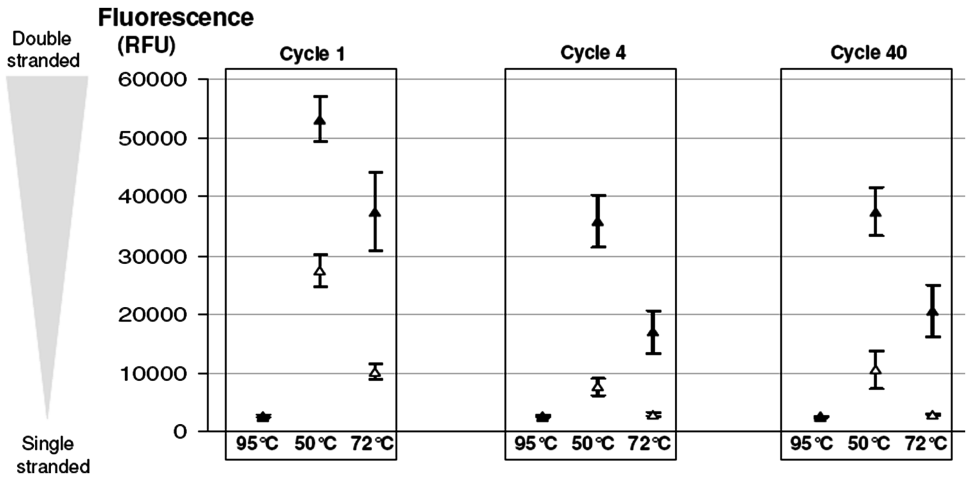

Figure 5. Real-time readings of SG I fluorescence due to 20-mer DNA hybridization. At cyclic temperatures typical of a PCR after 1, 4 and 40 cycles under non-crowded (open symbols) and MMC (solid symbols), MMC yielded fluorescence signals that were upto 3-fold and 8-fold higher than the non-crowded condition at the annealing and extension phases, respectively. This trend was consistent when readings were compared after 1, 4 and 40 cycles that shows the sustainability of MMC effects over the entire 40 cycle period.

magnitude faster than macromolecules (Poly-Vinyl-Pyrrolidone: $7.9 \times 10^{-8}\,cm^2/s$; Ficoll: $13 \times 10^{-8}\,cm^2/s$). Therefore, it is reasonable to approximate the crowding model (solely in this context) by macromolecular confinement for *in silico* studies while noting the distinction between the phenomena. A recent study (3) provides an excellent mathematical relationship between the dimensions of a crowder with an equivalent confining spherical pore for enhancing protein refolding and a review (19) clarifies understanding of volume-exclusion-effects

by soluble macromolecules (MMC) as compared to that by fixed-boundary (Confinement). Our molecular modeling therefore provides a new way to study the effects of crowding by equivalent simple confinement models. Our experimental estimates of hybrid-populations at annealing and extension temperatures correlated well with simulation-based predictions of structural-distortion of helicity when length, sequence and type of nucleic-acid hybrids were varied, thus contributing to quantitative-mapping of *in silico to in vitro*. It is conceivable that *in vivo* the template DNA strand, a huge macromolecule of several megabases, might by itself provide a confinement effect.

We inferred from our simulations that the presence of more than one H-bond, and the lower RMSD of duplex DNA when heated under confinement conditions, indicate that the stability of DNA hybrids is enhanced irrespective of length, type (DNA/RNA) and sequence. The *in silico* target temperatures in our study were lower than *in vitro* temperatures of melting (T_m) and annealing since *in vitro* there are a much higher number of DNA molecules and it is known (by nearest-neighbour calculations) that for DNA the T_m and annealing temperatures are concentration-dependent, meaning that these temperatures decrease with decrease in the number of DNA in solution. Our simulations sufficiently show the essential principle behind confinement effects on thermally stabilizing double-strand DNA. Expanding our *in silico* model to simulate a finite number of DNA molecules (needing much higher computational power) could further enhance the correlation between *in silico* and *in vitro* experiments.

Moving to *in vitro* experiments we had the option between mono- and mixed crowding. From earlier work (14,20), we had an indication that mixed crowding might be more effective. We tested three different situations and found a correlation between increased molecular complexity of the crowding solution and increased stabilization of hybrids. The rationale for combining two or more different types of macromolecules in solution was to create shape and size anisotropy which is typical of *in vivo* systems. We combined PVP360, a random coil polymer with irregular shape with the globular Fc. Fc70, Fc400 and PVP360 have hydrodynamic radii of 5 nm, 13 nm and 20 nm, respectively (5). Such a mix has the potential to result in greater volume-exclusion effects than either of them alone (20). Our data supported these earlier findings by demonstrating greater stabilization and population of DNA hybrids under mixed crowding conditions than mono-crowders. Interestingly, the best working ratio of Fc400 to PVP360 concentration in our hands was ~10: 1 which is in good agreement with earlier data (21) on mixed crowding who found a ratio of 10: 1 between BSA (globular) and dextran (random coil polymer) the most effective in driving compact folding of lysozyme. Our data suggest that PVP360 can drive Fc70 into multimers and might be slowing down diffusion of both Fc400 and Fc70. Mixed crowding enables creation of pockets in-between bigger (slower-moving) crowders, thus mimicking an *in vivo* situation and facilitating formation of confined-spaces to enhance molecular association. This would explain an increased efficacy of mixed versus mono-crowding, however, more simulation work needs to be done to confirm this theory. Of note, our current 1 nanosecond simulations required approximately 200 hours computation time per-each simulation run in the MD Simulations program. These simulations predicted structural stabilization of DNA duplices under confinement and were validated by *in vitro* data. Longer simulations on finite number of DNA can make our observations on structural stabilization of DNA duplices under confinement more precise. Modelling of mixed crowding will demand far more computation time and greater computational power. *In vitro* work confirmed the *in silico* predictions, showing that MMC could stabilize nucleic acid structure as a double helix irrespective of length, sequence or type. Stabilizing effects of MMC on DNA:RNA hybrids may also partially explain its role in increasing cDNA yield of reverse transcriptase reactions by enhancing binding of oligo-dT primers to poly A sequence on mRNA independent of MMC effects on reverse transcriptase activity (14).

The CD spectra confirmed a loss of double helical DNA structure under non-crowded conditions at the PCR extension temperature, but its preservation under MMC (corroborating our melting curve data), suggests that mixed MMC of a routine PCR may provide more duplex-DNA substrate for *Taq* polymerase activity.

A central observation in our study is that in the absence of any other accessory molecules, MMC preferably promoted the hybridization of matching nucleotide hybridization over mismatches. Any non-specific promotion of nucleic acid hybridization was effectively ruled out by our experiments on oligomers containing single nucleotide polymorphisms in their sequences. Our data confirm earlier findings (8) that MMC enhances specificity of binding due to significant free energy differences of binding between mismatches and true matches, the latter being favoured by MMC. Their conclusions were largely based on measurements of melting temperatures of the DNA by biophysical methods. Our data shows that while there is specific enhancement of true matched hybrid annealing, there is also no non-specific enhancement of mismatch binding under mixed MMC. Further, our experiments with hair-pin forming single strands showed that under crowding, there was preferential formation of duplex-DNA by enhanced annealing of the single-stranded DNA leading to a 20-fold increment in the amount of duplices formed.

The above described effects point to the deciding factors in hybridization and enzymatic extension *in vitro*. Our *in vitro* study captured the initial non-enzymatic steps of a standard PCR tailored to yield amplicons at typically short annealing and extension times and not optimized techniques with dedicated hybridization buffers or long annealing times. The annealing phase of PCR is characterized by entropy-driven H-bond-dependent hybridization events between primers and template. In our real-time PCR setting, we found that annealing of oligomers was enhanced significantly by introducing crowders into the reaction environment.

Under non-crowded conditions, our data show that a significant 63% of annealed duplexes dissociated into single strands at the extension temperature. However, this drastic drop was grossly ameliorated by mixed MMC and only 29% of the annealed duplexes dissociated leaving behind 71% of intact duplexes at extension. However, at 95°C all DNA is single-stranded (±MMC) suggesting that crowding does not inhibit DNA-denaturation at 95°C (a requirement for successful PCR), the effects best seen at annealing and extension temperatures. Therefore the temperature-dependent nature of crowding effects selectively enhances specific DNA hybridization without compromising on key PCR requirements.

From these observations, we therefore infer, that under non-crowded conditions, annealing behaves as a highly random event and it is likely that not all primers find their complementary bases and even those bound may not be stable under the routine extension temperatures. Crowding that favours macromolecular association and lowers conformational entropy (i.e. the structural randomness of the system), could help in enhancing and stabilizing greater, specific primer-template binding in these conditions. In extension of our earlier work (14) we have to conclude that the major effects of MMC on PCR do not lie in the thermoprotection of the polymerase but in increasing the yield of the extension phases from the very first cycle on.

Our findings have a bearing on the understanding of biochemical reactions *in vivo*. It is conceivable that *in vivo* the template DNA strand, a huge macromolecule (several megabases long), by itself might provide a confinement effect as described above. It is interesting to note that the confining macromolecules used for our simulations resemble cycloamylose-like structures. Cycloamylose carbohydrate polymers (22) have been suggested to be one of the factors that stabilize proteins against heat (23,24) in thermophiles and hyperthermophiles, micro-organisms that have evolved in harsh environments with temperatures from 80°C to 150°C. In the absence of published work, our *in silico* data suggest that crowding may also stabilize the nucleic acid material in these thermophiles, and that cycloamylose may play this role in thermophiles. Furthermore, we calculated that for our real-time hybridization experiments, the total fraction volume occupancy was 22% under mixed MMC. This is within the range of biological crowding that is found in the cell cytoplasm (25) (5–40%) and the nucleus (3) (10–40% volume occupancy).

In conclusion, MMC and Macromolecular Confinement are important parameters for successful nucleotide hybridization events both *in vitro* and *in vivo*. The ability of MMC to preferably drive perfect nucleotide matches in the absence of accessory molecules suggests an ancient role of MMC in the evolution of replication and transcription and a contemporary role in the improvement of widely spread DNA amplification techniques *in vitro*.

SUPPLEMENTARY DATA

Supplementary Data are available at NAR Online.

FUNDING

Singapore-MIT-Alliance (SMA) and a proof of concept grant by the Economic Development Board of Singapore; Raine Medical Foundation (University of Western Australia, Perth) to M.R; the NUS Tissue Engineering Programme is gratefully acknowledged. Funding for open access charge: Personal Resources/ SMA-NUS.

Conflict of interest statement. None declared.

REFERENCES

1. Ellis,R.J. (2001) Macromolecular crowding: an important but neglected aspect of the intracellular environment. *Curr. Opinion Struct. Biol.*, **11**, 114–119.
2. Partikian,A., Ölveczky,B., Swaminathan,R., Li,Y. and Verkman,A.S. (1998) Rapid diffusion of green fluorescent protein in the mitochondrial matrix. *J. Cell Biol.*, **140**, 821–829.
3. Cheung,M.S., Klimov,D. and Thirumalai,D. (2005) Molecular crowding enhances native state stability and refolding rates of globular proteins. *PNAS*, **102**, 4753–4758.
4. Hancock,R. (2004) A role for macromolecular crowding effects in the assembly and function of compartments in the nucleus. *J. Struct. Biol.*, **146**, 281–290.
5. Harve,K.S., Lareu,R.R., Rajagopalan,R. and Raghunath,M. (2006) Macromolecular crowding in biological systems: dynamic light scattering (DLS) to quantify the excluded volume effect. *Biophys. Rev. Lett.*, **1**, 317–325.
6. Zimmerman,S.B. and Harrison,B. (1987) Macromolecular crowding increases binding of DNA polymerase to DNA: an adaptive effect. *Proc. Natl Acad. Sci. USA*, **84**, 1871–1875.
7. Munishkina,L.A., Cooper,A.M., Uversky,V.N. and Fink,A.L. (2004) The effect of macromolecular crowding on protein aggregation and amyloid fibril formation. *J. Mol.Recogn.*, **17**, 1–9.
8. Goobes,R., Kahana,N., Cohen,O. and Minsky,A. (2003) Metabolic buffering exerted by macromolecular crowding on DNA-DNA interactions: origin and physiological significance. *Biochem.*, **42**, 2431–2440.
9. Bird,L., Subramanya,H.S. and Wigley,D.B. (1998) "Helicases: a unifying structural theme?" *Curr. Op. Struct. Biol.*, **8**, 14–18.
10. Johnson,D.S., Bai,L., Smith,B.Y., Patel,S.S. and Wang,M.D. (2007) Single-molecule studies reveal dynamics of DNA unwinding by the ring-shaped T7 helicase. *Cell*, **29**, 1299–1309.
11. Ottiger,H.-P. and Hubscher,U. (1984) Mammalian DNA polymerase a holoenzyme with possible functions at the leading and lagging strand of the replication fork. *PNAS*, **81**, 3993–3997.
12. Tucker,G.A. and Roberts,J.A. (2000) Methods in molecular biology: plant hormone protocols. *Humana Press*, **141**, 181–182.
13. Wilhelm,J., Hahn,M. and Pingoud,A. (2000) Influence of DNA. Target melting behaviour on real-time PCR quantification. *Clin. Chem.*, **46**, 1738–1743.
14. Lareu,R.R., Harve,K.S. and Raghunath,M. (2007) Emulating a crowded intracellular environment *in vitro* dramatically improves RT-PCR performance. *Biochem. Biophys. Res. Comm.*, **363**, 171–177.
15. Klimov,D.K., Newfield,D. and Thirumalai,D. (2002) Simulations of ß-hairpin folding confined to spherical pores using distributed computing. *PNAS*, **99**, 8019–8024.
16. Patel,M.M. and Anchordoquy,T.J. (2006) Ability of Spermine to differentiate between DNA sequences-preferential stabilization for A-tracts. *Biophys. Chem.*, **122**, 5–15.
17. Nkodo,A.E., Garnier,J.M., Tinland,B., Hongji,R., Desruisseaux,C., McCormick,L.C., Drouin,G. and Slater,G.W. (2001) Diffusion coefficient of DNA molecules during free solution electrophoresis. *Electrophoresis*, **22**, 2424–2432.
18. Woutersen,S., Mu,Y., Stock,G. and Hamm,P. (2001) Hydrogen-Bond lifetime measured by time-resolved 2D-IR spectroscopy: N-methyacetamide in methanol. *Chem. Phy.*, **266**, 137–147.

19. Zhou,H.-X., Rivas,G. and Minton,A.P. (2008) Macromolecular crowding and confinement; biochemical, biophysical and potential physiological consequences. *Annu. Rev. Biophys.*, **37**, 375–397.
20. Harve,K.S., Vigneshwar,R., Rajagopalan,R. and Raghunath,M. (2008) Macromolecular crowding as means of emulating cellular interiors *in vitro*: when less might be more. *PNAS*, **105**, E119.
21. Zhou,B.R., Liang,Y., Du,F., Zhou,Z. and Chen,J. (2004) Mixed macromolecular crowding accelerates the oxidative refolding of reduced, denatured lysozyme: implications for protein folding in intracellular environments. *J. Biol. Chem.*, **279**, 55109–55116.
22. Fujii,K., Minagawa,H., Terada,Y., Takaha,T., Kuriki,T., Shimada,J. and Kaneko,H. (2005) Use of random and saturation mutageneses to improve the properties of *Thermus aquaticus* amylomaltase for efficient production of cycloamyloses. *App. Env. Microbiol.*, **71**, 5823–5827.
23. Karantzeni,I., Ruiz,C., Liu,C. and Licata,V.J. (2003) Comparative thermal denaturation of Thermus aquaticus and Escherichia coli type 1 DNA polymerases. *Biochem J.*, **374**, 785–792.
24. Sterner,R. and Liebl,W. (2001) Thermophilic adaptation of proteins. *Crit. Rev.Biochem. Mol. Biol.*, **36**, 39–106.
25. Ellis,R.J. and Minton,A.P. (2003) Join the crowd. *Nature*, **425**, 27–28.